Desalination and Water Treatment
www.deswater.com

doi: 10.5004/dwt.2019.23616

146 (2019) 351–361
April

Study on adsorption of terramycini hydrochloride from aquaculture wastewater using modified activated carbon fiber

Xiaocai Yu*, Hang Yang, Jinghua Liu, Liping Wang, Meichen Guo

College of Marine Science and Environment, Dalian Ocean University, Dalian 116000, China, Tel. 86 13842606059; email: 978404210@qq.com (X. Yu), Tel. 86 18041156682; email: yanghang951012@163.com (H. Yang), Tel. 86 07392719366; email: 593809434@qq.com (J. Liu), Tel. 86 18975486999; email: 2727619686@qq.com (L. Wang), Tel. 86 18973999269; email: 1146176981@qq.com (M. Guo)

Received 14 April 2018; Accepted 14 December 2018

ABSTRACT

Activated carbon fiber (ACF) was modified by sulfuric acid impregnation method and used as an adsorbent for terramycini hydrochloride (TH). The structural and chemical properties of modified activated carbon fiber were characterized by SEM, FTIR, EDS and BET analysis methods. Six factors (namely, modification time, dosage of ACF, initial concentration of TH, adsorption time, pH value and interfering ion) were screened to study their effects on the adsorption of TH onto modified ACF. A 16 full factorial design was employed for optimizing the adsorption condition. The removal of TH reached 93% under the optimal condition: modification time of 45 min, solution pH of 6, adsorbent dose of 0.6 g L^{-1}, 3 h of reaction time and 15 mg L^{-1} of initial concentration of TH. The dosage of adsorbent had the most positive effect on the removal of TH. The adsorption kinetic data were fitted well by pseudo-second order model. The adsorption isotherm data were favored to Langmuir model with the maximum adsorption capacity of 99.3 mg g^{-1}. The regeneration of saturated modified ACF was studied using NaOH as the regeneration reagent. The present work shows that the modified ACF was a good adsorbent for TH removal from aquaculture wastewater.

Keywords: Activated carbon fiber; Adsorption; Antibiotic

1. Introduction

Antibiotics are medicines used extensively in the fields of veterinary and aquaculture to enhance growth and control disease [1,2]. With increasing attention to environmental protection, antibiotics have become emergent global environment concern. So far, a variety of antibiotics and their metabolites had been detected in seawater [3,4]. The misuse of antibiotics generated bacterial resistance to the antibiotics, even posed a potential threat to human and animal health [5,6]. Therefore, it is necessary to take some effective measures to remove antibiotics from contaminated water. In terms of the quantity of production and use, tetracycline (TC) is the second most popular antibiotic for several decades. Terramycini hydrochloride (TH), whose structure is shown as Fig. 1 studied in this paper is one kind of tetracycline.

The mainstream methods, including adsorption [7,8], Fenton oxidation [9,10], electrochemical oxidation [11,12], biological degradation [13] and photocatalysis oxidation [6,14] have been employed for TH removal. Nowadays, (chemical or physical) adsorption has been considered as the most effective and facile technique for antibiotics removal from wastewater [15]. Up to now, various kinds of adsorbents, including graphene oxide [16], natural zeolite [17], activated carbon [18] and so on, have been developed for this purpose.

Activated carbon fiber (ACF) is a novel and efficient adsorbent. Compared with the traditional granular activated

* Corresponding author.

carbon, ACF has a more large specific surface area and rich micropores. So far, it has been widely used in chemical industry, environmental protection, catalysis, medicine, electronic industry, food hygiene and other fields [19–22]. Many studies indicated that ACF is an effective adsorbent for many pollutants, several studies have been performed aiming to investigate the adsorption of organic compounds and heavy metals on ACF [23–26]. Meanwhile, many researches also indicated that the adsorption ability of ACF can be enhanced evidently by several methods of modification, including microwave modification, acid modification and metal modification [27–29]. In this paper, ACF was modified using sulfuric acid impregnation method.

The aims of this study were to (1) investigate the characterization of modified ACF by BET, EDS, FTIR and SEM analysis methods; (2) evaluate the effects of six factors on the removal rate of TH from aquaculture wastewater by batch experiments; (3) study the optimal experiment condition using orthogonal test; (4) explore the adsorption isotherm and kinetics to determine the adsorption mechanism; (5) test the reusability of modified ACF using NaOH as regeneration reagent.

2. Experimental setup

2.1. Materials and instruments

ACF (ST-1300) was provided by Jiangsu Nantong Fiber Industry Co., China. All reagents employed include: terramycini hydrochloride, NaOH, H_2SO_4, NaCl, $(NH_4)_2SO_4$, $NaNO_3$ and KH_2PO_4. The stock solution to TH was configured using seawater from aquaculture area in Dalian Ocean University, China.

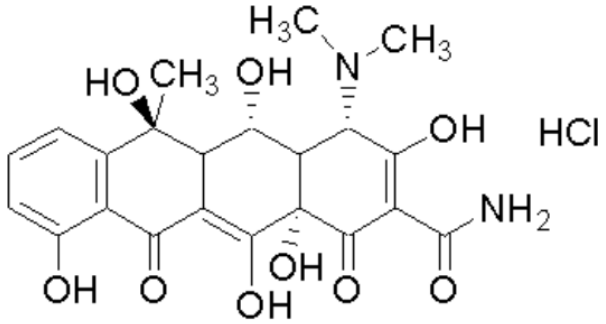

Fig. 1. Molecular structure of TH.

The spectrophotometric measurements were made with UV–Vis spectrometer (SP-752). Surface area analysis and distribution of pore size analysis were performed on high speed automatic specific surface area instrument (Quantachrome 3.0, America). The SEM and FTIR analysis were performed using field emission scanning electron microscope (SU 1510) and FTIR spectrometer (FTIR-650), respectively. Furthermore, shaker (XB SHA-CA) and pH meter (Starter 3100, made in China) were used.

2.2. Pre-treating and modification of ACF

Pre-treatment: prior to the experiments, the ACF was sheared into fraction with size of 5 mm × 5 mm and then boiled in beaker using ultrapure water at 450°C for 1 h to remove organics and soluble salts on the surface of ACF. Then, the washed ACF was dried in oven at 100°C for 24 h [30].

Modification: the treated ACF was modified using 10% H_2SO_4 (50 mL/1 g ACF) on shaker (100 rpm, 70°C) for 15, 30, 45, 60, 75 and 90 min, respectively, then the modified ACF was washed using ultrapure water and dried in oven at 100°C for 24 h.

2.3. Batch experiments and orthogonal test

The batch experiments all were carried out in 250 mL flasks containing 50 mL of simulated solution. pH was adjusted using H_2SO_4 and NaOH. The flask was shaken in shaker at 150 rpm and 298 K. Aqueous samples were filtrated using filter paper and the concentrations of TH in the solution were analyzed after reaction. The details of the experimental conditions are presented in Table 1. In addition, an orthogonal test with five factors and four levels was carried out. The determination of experimental conditions refers to the previous literature [31,32].

2.4. Adsorption kinetics

Adsorption kinetics study was carried out by shaking 0.12 g of the adsorbents in flask containing 200 mL of TH solutions with an initial concentration of 20, 30, 40 mg L^{-1} (at pH 8, 25°C). After pre-determined reaction time (10; 20; 30; 40; 50; 60; 120; 240; 300; 360; 1,440; 2,880; 5,760 min), the aqueous samples were filtered, and the concentration of TH in the solution was determined. Pseudo-first-order, pseudo-second-order, Elovich and intra-particle diffusivity equations [33–36] were used for modeling the adsorption kinetics (Eqs. (1)–(4)).

Table 1
Experimental conditions

Set	Aim of experiment	Modification time of ACF (min)	TH concentration (mg L^{-1})	Adsorbent dosage (g)	Reaction time (min)	pH
1	Effect of modification time	0–75	20	0.02	360	8
2	Effect of adsorbent dosage	45	20	0.01–0.06	360	8
3	Effect of TH concentration	45	5–30	0.03	360	8
4	Effect of reaction time	45	20	0.03	60–360	8
5	Effect of pH	45	20	0.03	360	5–10
6	Effects of presence of Na^+, NH_4^+, NO_3, and $H_2PO_4^-$ ion	45	20	0.03	360	8

$$q_t = q_e\left(1 - e^{(-k_1 t)}\right) \quad (1)$$

$$\frac{t}{q_t} = \frac{1}{k_2 q_e^{\,2}} + \frac{t}{q_e} \quad (2)$$

$$q_t = (1/\beta)\ln(\alpha/\beta) + (1/\beta)\ln(t) \quad (3)$$

$$q_t = k_w t^{0.5} + b \quad (4)$$

Among the constants, t is the reaction time (min), q_e is the amount of TH adsorbed on ACF (mg·g^{-1}) at equilibrium and q_t is the amount of TH adsorbed at given time t (mg·g^{-1}). k_1 is the pseudo-first-order constant, k_2 is the pseudo-second-order constant. α and β are Elovich constants, k_w and b are intra-particle diffusivity constants.

2.5. Adsorption isotherms

The adsorption isotherms were investigated by shaking 0.03 g of the adsorbents in flask containing 50 mL of TH solutions with varying initial concentration from 5 to 200 mg L^{-1} (25°C, pH 8, shaking 24 h and 150 rpm). The equilibrium data were fitted by Langmuir and Freundlich isotherm models [37,38] (Eqs. (5) and (6)).

$$\frac{c_e}{q_e} = \frac{1}{(k_l \times q_m)} + \frac{c_e}{q_m} \quad (5)$$

$$q_e = k_f c_e^{\,n} \quad (6)$$

The constant q_m is the maximum adsorption capacity (mg g^{-1}). The constants k_l and k_f are Langmuir and Freundlich constants, respectively, and calculated from the intercept and slope of equations.

2.6. Determination of TH concentration

The concentration of TH was determined by ultraviolet spectrometer at λ_{max} value of TH (275 nm wavelength). The amount of TH adsorbed (mg g^{-1}) was calculated based on a mass balance equation as given in Eq. (7) and the degradation rate was calculated as given in Eq. (8):

$$q_e = \frac{(C_o - C_e)V}{W} \quad (7)$$

$$\text{Degradation rate} = \frac{c_0 - c_e}{c_0} \times 100 \quad (8)$$

Among the constants, q_e is the amount of TH adsorbed on ACF (mg g^{-1}); c_o is the initial concentration of TH in the solution (mg L^{-1}); c_e is the concentration of TH in the solution at equilibrium (mg L^{-1}); V is the volume of the solution (L) and W is the dosage of the ACF (g).

2.7. Regeneration of saturated modified ACF

The regeneration of saturated modified ACF was studied using solvent regeneration method. 1 mol L^{-1} NaOH was employed as the regeneration agent to regenerate the saturated ACF. The regeneration was performed by shaking 1 g saturated ACF in flask containing 100 mL of NaOH solutions (25°C, shaking 1 h and 150 rpm). The calculation of regeneration rate was based on the equation as given in Eq. (9) as follows:

$$\text{Regeneration rate} = \frac{q_n}{q_m} \quad (9)$$

where n is the times of use and q_n is the adsorption capacity (mg L^{-1}) at the n times. q_m is the maximum adsorption capacity, 99 mg g^{-1}.

3. Results and discussion

3.1. Characterization of ACF

The characterized samples were ACF modified for 45 min and origin ACF.

FTIR spectrum is employed to define the active chemical groups present on the ACF surfaces. The FTIR spectra of tested ACF ranged from 400 to 4,000 cm^{-1} are illustrated in Fig. 2, a broad band at 3,428 cm^{-1} which was assigned to the O–H stretching vibrations, indicating the presence of surface hydroxylic groups and chemisorbed water. After modification, a peak at 2,922 cm^{-1} which was ascribed to C–H stretching vibrations appeared, indicating the presence of alkane/alkene groups on the surface of ACF.

The micrographs are used to reveal fractures in the solid surface. The surface micrographs of ACF obtained by SEM at ×1,000 magnification are given in Fig. 3. Compared with the original ACF, the surface of the modified ACF had no evident difference. This could conclude that the acid modification almost did not affect the surface structure of ACF. Both ACF and modified ACF show homogeneous surface morphology with presence of pitch on their surface.

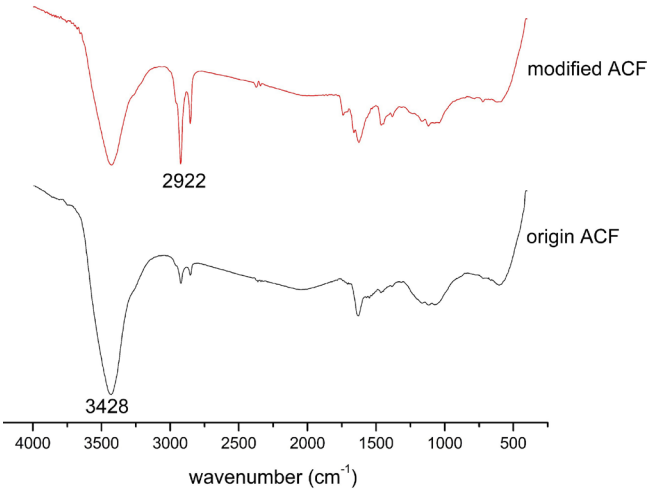

Fig. 2. FTIR spectrum of ACF (original and modified).

The nitrogen adsorption isotherms of ACF were studied and the results were shown in Fig. 4. The BET surface area, micro-pore volume and average diameter of samples were summarized in Table 2. Based on the guidelines reported for BDDT classification [39], the nitrogen adsorption isotherms of ACF and modified ACF both belong to the BDDT type I classification, corresponding to the typical microporous material. Fig. 4(a) indicates the N_2 adsorption capacity of modified ACF was greater than ACF. Fig. 4(b) shows the pore size distribution of modified ACF and ACF both were dominated by micropores. Table 2 shows ACF's surface area and micro pore volume increased after modification, since pores were partially unfolded by sulfuric acid modification, resulting in the increase of surface pore and specific area.

Table 3 shows the proximate analysis of ACF. The results indicate that modified ACF has higher amount of fixed carbon, indicating the higher adsorption capacity. Fig. 5 shows the EDS analysis of ACF, the results reveal: (i) O and C were the major element and P and Na were minor element for the composition of ACF; (ii) after modification, the content percentage of C increased and that of other elements decreased, indicating the increase in the carbon-containing functional groups and decrease in the oxygen-containing functional groups on the surfaces of the ACF.

Table 2
Surface properties of ACF (original, modified)

Samples	S_{BET} ($m^2\ g^{-1}$)	V_{micro} (cc g^{-1})	$D_{average}$ (nm)
ACF	848.012	0.347	3.829
Modified ACF	1,227.218	0.43	3.413

Table 3
Proximate analysis of ACF (original, modified)

Samples	Ash (%)	Moisture (%)	Volatile matter (%)	Fix carbon (%)
ACF	1.5	<0.1	3.4	95.0
Modified ACF	0.4	<0.1	0.9	98.6

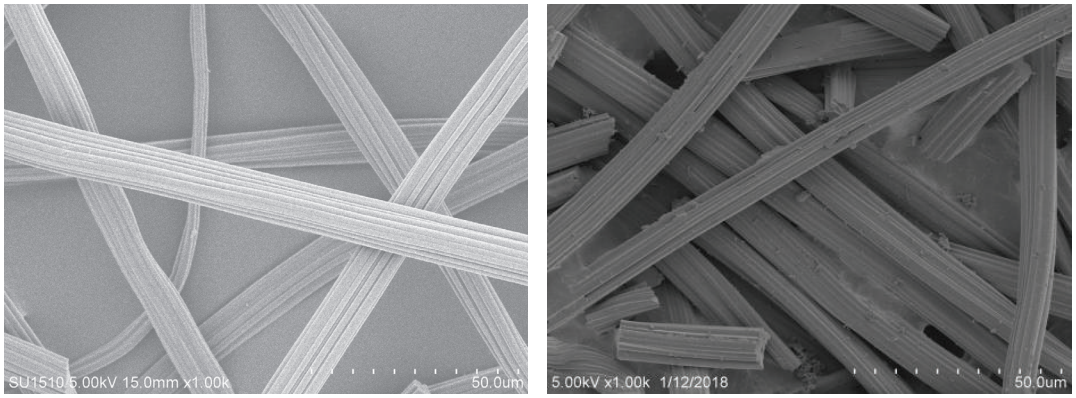

Fig. 3. SEM characterization of ACF (original (a) and modified (b)).

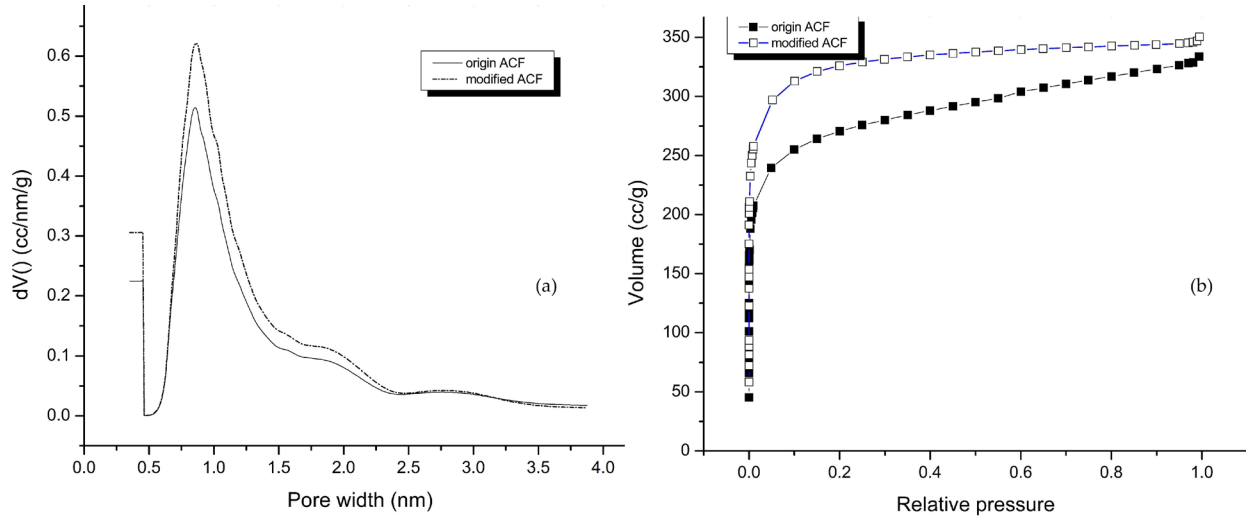

Fig. 4. N_2 adsorption isotherms (a) and distribution of pore size (b) of ACF (original, modified).

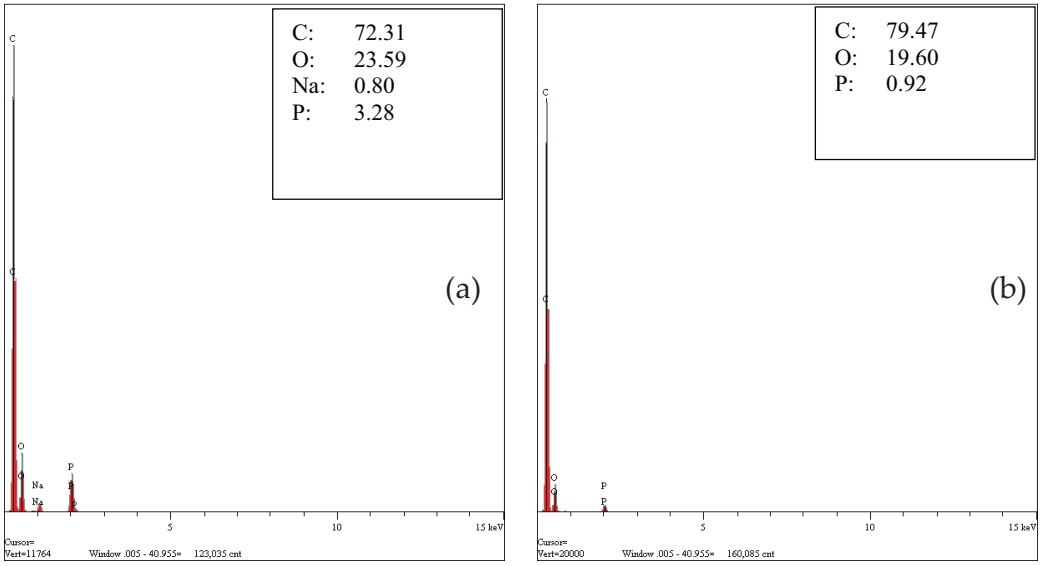

Fig. 5. EDS characterization of ACF (original (a), modified (b)).

3.2. Batch experiments and orthogonal test

Fig. 6(a) indicates the effect of modification time on TH adsorption when the modification time varied from 0 to 90 min. The results show: (i) the adsorption capacity of TH was 21.3 mg g^{-1} using unmodified ACF and the adsorption capacity of ACF for TH was enhanced by sulfuric acid modification, since modification unfolded the pore on the surface of ACF, which enhanced the adsorption capacity of ACF; (ii) the degradation rate and unit adsorption quantity reached the peak, 63% and 31 mg g^{-1}, respectively, when modification time was 45 min; (iii) overtime modification was not conducive to the adsorption of TH, since overtime modification may be harmful to the surface of ACF, resulting in the decrease of adsorption capacity. Therefore, modification time of 45 min was selected as experimental parameter for the rest of the experiments.

Fig. 6(b) indicates the effect of dosage of modified ACF on TH adsorption when the dosage varied from 0.01 to 0.06 g. The results show: (i) the unit adsorption quantity increased and decreased consequently with the increase of dosage since saturation of sites and solid aggregation due to particle–particle interaction; (ii) the degradation rate increased with the increase of dosage; (iii) the degradation rate reached the peak, 97%, when the dosage was 0.04 g. This behavior was attributed to the availability of more number of vacant surface sites and large surface area with the increasing dosage, which resulted in the increase in the degradation rate of TH [40]. Therefore, dosage of 0.03 g was selected as experimental parameter for the rest of the experiments.

Fig. 6(c) indicates the effect of initial concentration of TH on TH removal when the initial concentration of TH was 5–30 mg L^{-1}. The results show: (i) the unit adsorption quantity increased with the increase of dosage; (ii) the degradation rate increased and decreased consequently with the increase of dosage; (iii) the degradation rate reached the peak, 94%, when the concentration of TH was 15 mg L^{-1}. To the best of our knowledge, the unit adsorption quantity of TH depends upon the ratio of the number of adsorbate moiety to the available active sites of modified ACF. The larger value of this ratio corresponds to the higher unit adsorption quantity of TH, which was consistent with other literature [41]. However, at low concentration, the degradation rate increased with increasing concentration, which was not consistent with relative literature [42]. This may be attributed to the low driving force and concentration gradient at low concentration, resulting in a low degradation rate. Therefore, concentration of 20 mg L^{-1} was selected as the experimental parameter for the rest of the experiments.

Fig. 6(d) indicates the effect of reaction time on TH removal when reaction time was 1–6 h. As a result, the degradation rate and unit adsorption quantity increased with the increase in reaction time and reached maximum, 92% and 30.7 mg g^{-1}, respectively, after 6 h of reaction. The details could be discussed later in kinetics. Therefore, reaction time of 6 h was selected as experimental parameter for the rest of the experiments.

Fig. 6(e) indicates the effect of pH on TH adsorption when pH was 5–10. The results show the degradation rate and unit adsorption quantity both decreased with the increase of pH and reached peak, 96% and 32.1 mg g^{-1}, respectively, when pH was 5. The adsorption of TH is generally recognized to be favored at lower acidic pH values due to two factors: (i) TH possesses multiple ionizable functional groups, mainly corresponding to three acid dissociation constants (pK a = 3.6, 7.5 and 9.4), respectively. Therefore, TH exists as a cationic (pH < 3.6), zwitterionic (3.6 < pH < 7.5), and anionic (pH > 7.5) species under varied pH value. (ii) Many studies indicate the surface of modified ACF may carry negative charge, which increases with the increase of pH value. Therefore, the adsorption of TH on modified ACF was driven mainly by electrostatic attraction when pH < 3.6 and driven mainly by electrostatic repulsion when pH > 7.5. In addition, given the objective studied in this paper is TH from aquaculture wastewater, in which common pH value is 8. Good efficiency of removal still was obtained at pH 8, indicating the modified ACF could be employed to the practical

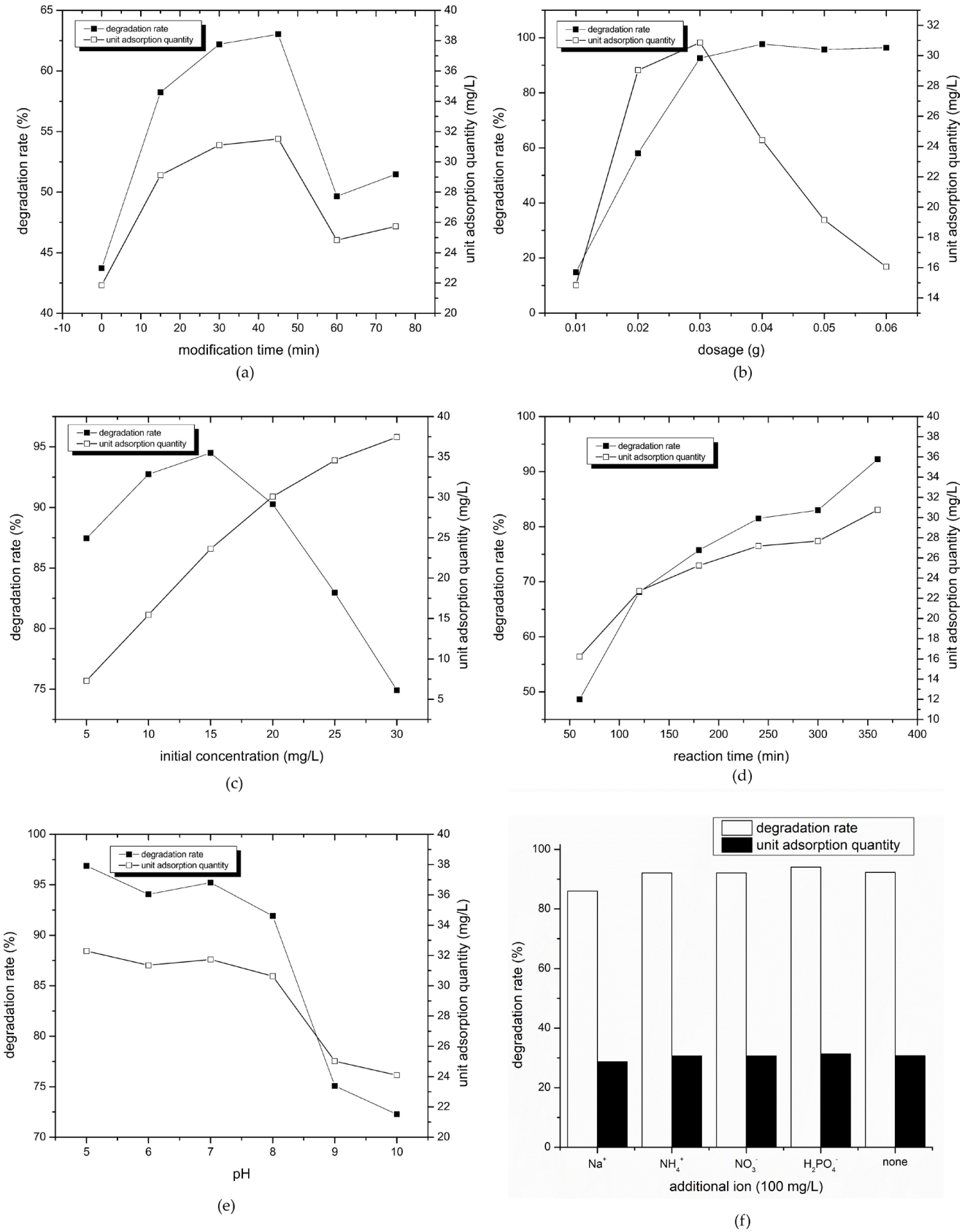

Fig. 6. Effects of different factors on the adsorption of TH (modification time (a), dosage (b), initial concentration (c), reaction time (d), pH (e), additional ions (f)).

treatment of TH in aquaculture wastewater. Therefore, pH at 8 was selected as the experimental parameter for the rest of the experiments.

Fig. 6(g) indicates the effect of interfering ion, including extra Na^+, NH_4^+, NO_3^-, $H_2PO_4^-$ ions, on the TH removal. The results show: (i) the presence of common non-metallic substances from aquaculture wastewater, such as NH_4^+, NO_3^-, $H_2PO_4^-$, have no evident effect on the adsorption of TH; (ii) the presence of Na^+ ion has the certain negative effect on the adsorption of TH. This trend may be attributed to two factors: (i) the presence of Na^+ ion had the competitive adsorption effect on TH; (ii) the Na^+ ion may form a complex with TH, which was more difficult to be adsorbed on ACF than TH, resulting in the decrease of degradation rate.

Table 4 shows the orthogonal experiment table. The optimal conditions for TH removal were determined by orthogonal experiment and shown as following: 45 min of modified time, 0.03 g of dosage, 15 mg L^{-1} of initial concentration of TH, 3 h of reaction time and pH value at 6. Under the optimal condition, the removal rate and unit adsorption quantity of TH reached 93%, 23.35 mg g^{-1}, respectively. In addition, the influence order for the each factors was obtained as following: ACF dosage > initial concentration of TH > pH≈ modification time of ACF > reaction time.

3.3. Adsorption kinetics

Fig. 7 shows the pseudo-first-order (a), pseudo-second-order (b), Elovich (c) and intraparticle diffusivity (d) kinetic models plots, respectively. Table 5 provides the evaluated parameters of all kinetic models. The experimental data fitted well with pseudo-second-order (b), Elovich (c) and intraparticle diffusivity (d) models.

As shown in Table 5, all correlation coefficients R^2 of first-order kinetic model were low and the theoretical q_e values calculated are not consistent with the experimental values q_e, indicating the adsorption process did not follow the pseudo-first-order model.

The pseudo-second-order kinetic model has been employed to explain the kinetic adsorption of the antibiotics onto the carbon material [40]. Fig. 7(b) shows the pseudo-second-order kinetic fitting line. The experimental data q_e was consistent well with the calculated values and the correlation coefficients R^2 of pseudo-second-order fitting are all close to 1 as shown in Table 5, which indicates the adsorption process can described by pseudo-second-order model.

The Elovich model has been employed to assume the heterogeneous distribution of surface adsorption energy and reflect the existence of different active adsorption sites on irregular surfaces. The fitting correlation coefficients R^2 are close to 1 at the first phase as shown in Table 5, indicating the adsorption behavior of TH on modified ACF is consistent with Elovich model.

The intraparticle diffusivity model is used to analyze the adsorption mechanism, including the adsorption rate and possible rate-limiting steps of the reaction process [43]. Fig. 7(d) shows the plot of intraparticle diffusivity model, indicating that the adsorption behavior was controlled by two phases [44]. In the first phase, the plots are close to the

Table 4
Orthogonal test table

Order	Modification time (min)	Dosage of ACF (g)	Initial concentration of TH (mg L^{-1})	Adsorption time (h)	pH value	Degradation rate (%)	Unit adsorption quantity (mg g^{-1})
1	15	0.01	10	3	6	16.49	8.25
2	30	0.01	15	4	7	30.24	22.68
3	45	0.01	20	5	8	20.29	20.29
4	60	0.01	25	6	9	19.86	24.82
5	45	0.02	10	4	9	63.69	15.92
6	60	0.02	15	3	8	41.91	15.71
7	15	0.02	20	6	7	50.65	25.33
8	30	0.02	25	5	6	34.64	21.65
9	60	0.03	10	5	7	82.84	13.81
10	45	0.03	15	3	6	93.40	23.35
11	30	0.03	20	6	9	76.56	25.52
12	15	0.03	25	4	8	60.52	25.22
13	30	0.04	10	6	8	91.75	11.47
14	15	0.04	15	5	9	91.86	17.22
15	60	0.04	20	4	6	88.45	22.11
16	45	0.04	25	3	7	79.80	24.94
K1	219.52	86.87	254.76	219.52	232.98		
K2	233.20	190.89	257.40	242.90	243.53		
K3	257.17	313.32	235.95	229.62	214.46		
K4	233.04	351.85	194.82	238.82	251.97		
R	37.65	264.97	62.58	23.38	37.50		

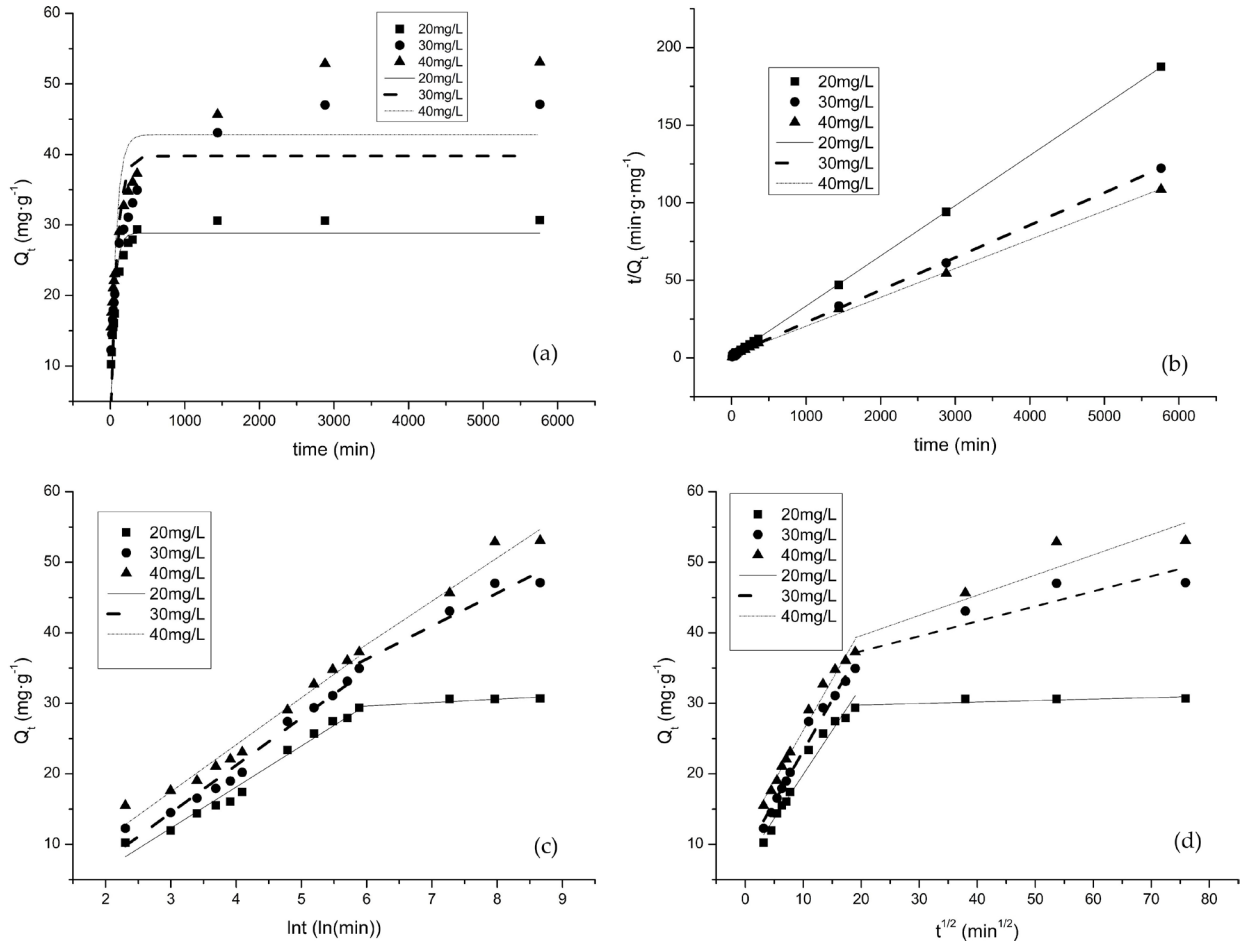

Fig. 7. Pseudo-first-order (a), pseudo-second-order (b), Elovich (c) and intraparticle diffusivity (d) model plots for TH (20, 30, 40 mg L^{-1}) adsorption onto modified ACF.

Table 5
Kinetic model parameters for TH adsorption onto modified ACF

Kinetic parameters	20 mg L^{-1}		30 mg L^{-1}		40 mg L^{-1}	
Pseudo-first-order model						
k_1 (min^{-1})	0.043		0.027		0.32	
q_m (mg g^{-1})	28.85		39.77		42.79	
R^2	0.8996		0.7790		0.6971	
Pseudo-second-order model						
q_e (mg g^{-1})	30.91		47.80		53.76	
k_2 (g mg^{-1} min^{-1})	1.0×10^{-3}		2.3×10^{-4}		1.9×10^{-4}	
R^2	0.9999		0.9993		0.9984	
Elovich model						
B (g mg^{-1})	0.17	2.08	0.14	0.21	0.15	0.16
A (g min^{-1} mg^{-1})	0.07	0	0.063	1.26	0.10	0.20
R^2	0.9765	0.7348	0.9734	0.9036	0.9716	0.9196
Intraparticle diffusivity model						
k_w (min^{-1})	1.24	0.020	1.45	0.21	1.44	0.28
b	7.44	29.34	8.74	33.13	11.75	33.87
R^2	0.9659	0.4757	0.9773	0.7059	0.9814	0.7801

origin, which indicated that the adsorption rate was faster and the rate step was controlled mainly by intraparticle diffusion. In the later stage, the fitting line segment is deviated from the origin and the linear intercept b is larger, which indicated the step of the adsorption rate was controlled by membrane diffusion. This behavior may be due to three factors: (i) the diffusion pores of modified ACF became saturated with the process of adsorption; (ii) the electrostatic repulsion of the modified ACF increased and (iii) the TH concentration reduced during the adsorption process.

3.4. Isotherms

Fig. 8 shows the Langmuir (a) and Freundlich (b) models plots for the adsorption of TH onto modified ACF. The adsorption isotherm parameters obtained from the models were given in Table 6.

Langmuir model assumes the homogeneous adsorption and monolayer adsorption on the surface of adsorbent. As shown in Table 6, Langmuir model exhibits a stronger fitness ($R^2 > 0.998$), which indicates the adsorption process well follows the Langmuir model. In addition, the parameter k_l obtained indicates the adsorption process belongs to favorable adsorption (when k_l is between 0 and 1). The maximum adsorption capacity q_m, 99.3 mg g^{-1}, is calculated from Langmuir equation. The Freundlich model assumes heterogeneous adsorption on the surface of adsorbent. As shown in Table 4, the correlation coefficients R^2 is lower compared with Langmuir model, which suggested the inapplicability of Freundlich model to describe the adsorption behavior of TH on modified ACF.

Furthermore, a comparison has been employed for the adsorption capacities of different adsorbents for TH as presented in Table 7. The table shows the q_m obtained using modified ACF was not very high compared with other adsorbents. This is due to that the configured solution of TH in this paper was derived directly from aquaculture wastewater, in which many interfering ions exist and 99.3 mg g^{-1} of q_m was achieved. This could indicate the modified ACF is a promising adsorbent for TH removal from aquaculture wastewater.

3.5. Regeneration of ACF

Compared with traditional activated carbon, the cost using ACF as adsorbent is more expensive. Therefore, it is necessary to regenerate the depleted ACF using an appropriate method. In this paper, the solvent regeneration method was employed to activate saturated ACF, which is a common method of carbon material regeneration. Herein, the regeneration of saturated ACF was investigated using NaOH as regeneration agent. Fig. 9 shows the regeneration effect of saturated modified ACF. The results reveal that the regeneration rate decreased with increasing regeneration times and it reached 58% after six times regeneration. In addition, though certain effects have been obtained using NaOH as regeneration agent, the better method of regeneration remains to be developed.

Table 6
Isotherm parameters for TH adsorption on modified ACF

Freundlich		Langmuir	
k_f (mg g^{-1})	23.92	k_l (L mg^{-1})	0.11
n	0.28	q_m (mg g^{-1})	99.30
R^2	0.9354	R^2	0.9833

Table 7
Maximum adsorption capacity (q_m) of various adsorbents for TH

Adsorbent	q_m (mg g^{-1})	Reference
Modified ACF	99.3	This study
Activated charcoal	518	[45]
Hydroxyapatite	291	[46]
Wetland substrates	280	[47]
Activated sludge	90.9	[48]

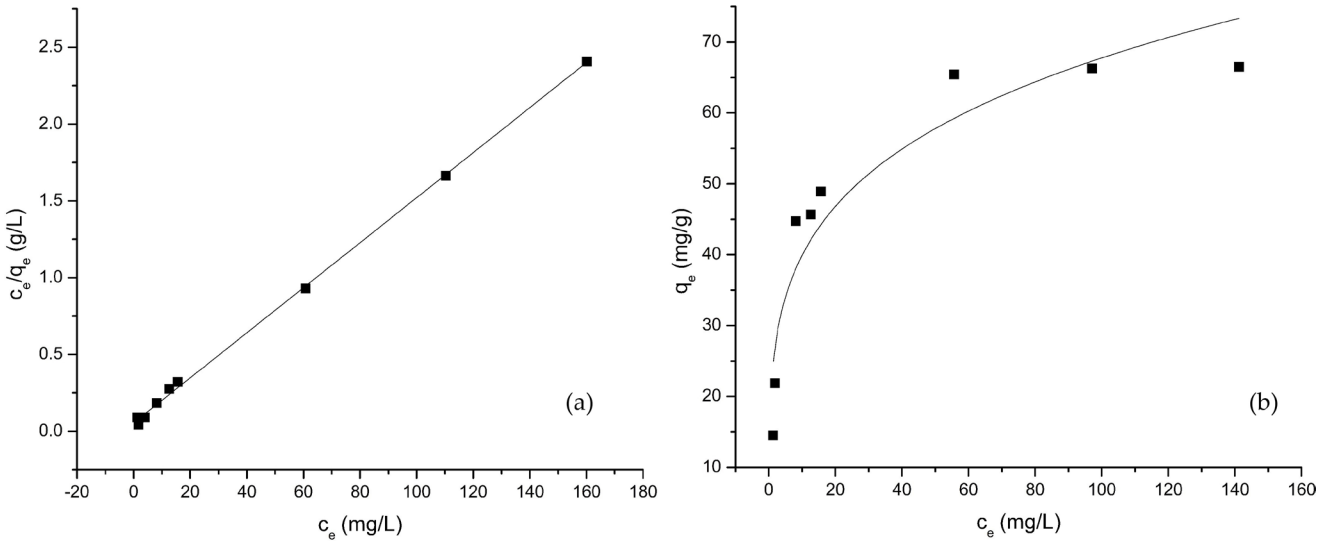

Fig. 8. Langmuir (a) and Freundlich (b) model plots for TH adsorption onto modified ACF.

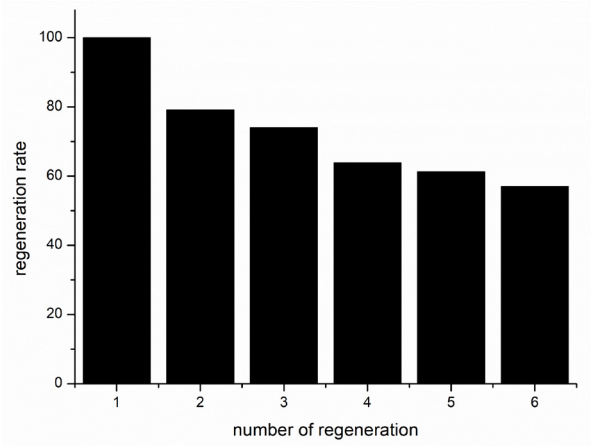

Fig. 9. Regeneration rate of saturated modified ACF.

4. Conclusion

After modified by sulfuric acid impregnation method, the specific area and micro volume of ACF were improved from 848 $m^2 g^{-1}$, 0.347 cc g^{-1} to 1,227 $m^2 g^{-1}$, 0.43 cc g^{-1}, respectively. Meanwhile, the results of SEM and EDS indicate by modification the surface of ACF had no obvious difference and the carbon-including function group increased relatively.

The single factors and orthogonal experiment for the adsorption of TH on ACF were tested. Under optimal conditions: modification of ACF at 45 min, dosage of ACF at 0.03 g, initial concentration of TH at 15 mg L^{-1}, reaction time at 3 h and pH value 6, the removal rate and unit adsorption quantity of TH reached 93%, 23.35 mg L^{-1}, respectively. In addition, the influence order for the each factors was obtained as follows: ACF dosage > initial concentration of TH > modification time of ACF ≈ pH value > reaction time.

The study of adsorption kinetics reveals that the pseudo-second-order kinetics accords with the adsorption behavior of TH on modified ACF. The study of adsorption isotherm shows that the adsorption behavior of TH on modified ACF is most fitted with Langmuir model with the maximum adsorption capacity at 99.3 mg g^{-1}, which indicates the adsorption behavior belongs to the monolayer adsorption. In addition, the regeneration of saturated ACF was tested. After six times of regeneration using NaOH as the regeneration agent, the regeneration rate still reached 58%.

Acknowledgments

The authors sincerely thank the funds for State Oceanic Administration marine nonprofit industry research and special project (No. 20130500), the subsidy for Liaoning Province Major Facilities Sharing Service Capacity Building Project (2016LD0105), the Liaoning Provincial Oceanic and Fishery Department research projects (No. 201733) for the financial support of this work.

References

[1] H. Long, S.F. Miller, C. Strauss, C. Zhao, L. Cheng, Z. Ye, K. Griffin, R. Te, H. Lee, C.C. Chen, Antibiotic treatment enhances the genome-wide mutation rate of target cells, Proc. Natl. Acad. Sci. U. S. A., 113 (2016) E2498–E2505.

[2] E.B. El Amari, E. Chamot, R. Auckenthaler, J.C. Pechère, D.C. Van, Influence of previous exposure to antibiotic therapy on the susceptibility pattern of Pseudomonas aeruginosa bacteremic isolates, Clin. Infect. Dis., 33 (2017) 1859–1864.

[3] W.J. Sim, J.W. Lee, E.S. Lee, S.K. Shin, S.R. Hwang, J.E. Oh, Occurrence and distribution of pharmaceuticals in wastewater from households, livestock farms, hospitals and pharmaceutical manufactures, Chemosphere, 82 (2011) 179–186.

[4] M.S. Díaz-Cruz, D. Barceló, Recent advances in LC-MS residue analysis of veterinary medicines in the terrestrial environment, Trac-Trends. in. Anal. Chem., 26 (2007) 637–646.

[5] J.S. Brugge, W. Yonemoto, A. Lustig, A. Golden, Adsorption of tetracycline and sulfamethoxazole on crop residue-derived ashes: implication for the relative importance of black carbon to soil sorption, Environ. Sci. Technol., 45 (2011) 5580–5586.

[6] R. Hao, X. Xiao, X. Zuo, J. Nan, W. Zhang, Efficient adsorption and visible-light photocatalytic degradation of tetracycline hydrochloride using mesoporous BiOI microspheres, J. Hazard. Mater., 209–210 (2012) 137–145.

[7] Z. Zhang, K. Sun, B. Gao, G. Zhang, X. Liu, Y. Zhao, Adsorption of tetracycline on soil and sediment: effects of pH and the presence of Cu(II), J. Hazard. Mater., 190 (2011) 856–862.

[8] H. Wu, H. Xie, G. He, Y. Guan, Y. Zhang, Effects of the pH and anions on the adsorption of tetracycline on iron-montmorillonite, Appl. Clay Sci., 119 (2016) 161–169.

[9] E. Elmolla, M. Chaudhuri, Optimization of Fenton process for treatment of amoxicillin, ampicillin and cloxacillin antibiotics in aqueous solution, J. Hazard. Mater., 170 (2009) 666–672.

[10] E.S. Elmolla, M. Chaudhuri, The feasibility of using combined Fenton-SBR for antibiotic wastewater treatment, Desalination, 285 (2012) 14–21.

[11] A. Dirany, I. Sirés, N. Oturan, A. Ozcan, M.A. Oturan, Electrochemical treatment of the antibiotic sulfachloropyridazine: kinetics, reaction pathways, and toxicity evolution, Environ. Sci. Technol., 46 (2012) 4074–4082.

[12] C.C. Jara, D. Fino, V. Specchia, G. Saracco, P. Spinelli, Electrochemical removal of antibiotics from wastewaters, Appl. Catal. B-Environ., 70 (2007) 479–487.

[13] S. Yahiat, F. Fourcade, S. Brosillon, A. Amrane, Removal of antibiotics by an integrated process coupling photocatalysis and biological treatment – Case of tetracycline and tylosin, Int. Biodeterior. Biodegrad., 65 (2011) 997–1003.

[14] Y. Zhao, B. Yin, G. Zhang, W. Shi, Facile fabrication of plate-like Bi3O4Cl for visible-light-driven photocatalytic degradation of tetracycline hydrochloride, Micro. Nano. Lett., 13 (2018) 9–11.

[15] R. Ocampo-Pérez, J. Rivera-Utrilla, C. Gómez-Pacheco, M. Sánchez-Polo, J.J. López-Peñalver, Kinetic study of tetracycline adsorption on sludge-derived adsorbents in aqueous phase, Chem. Eng. J., 213 (2012) 88–96.

[16] Y. Gao, Y. Li, L. Zhang, H. Huang, J. Hu, S.M. Shah, X. Su, Adsorption and removal of tetracycline antibiotics from aqueous solution by graphene oxide, J. Colloids Interface Sci., 368 (2012) 540–546.

[17] H.M. Otker, I. Akmehmetbalcioğlu, Adsorption and degradation of enrofloxacin, a veterinary antibiotic on natural zeolite, J. Hazard. Mater., 122 (2005) 251–258.

[18] J. Riverautrilla, G. Pradosjoya, M. Sánchezpolo, M.A. Ferrogarcía, I. Bautistatoledo, Removal of nitroimidazole antibiotics from aqueous solution by adsorption/bioadsorption on activated carbon, J. Hazard. Mater., 170 (2009) 298–305.

[19] S. Yang, T. Xiao, J. Zhang, Y. Chen, L. Li, Activated carbon fiber as heterogeneous catalyst of peroxymonosulfate activation for efficient degradation of Acid Orange 7 in aqueous solution, Sep. Purif. Technol., 143 (2015) 19–26.

[20] O.B. Yang, J.C. Kim, J.S. Lee, Y.G. Kim, Use of activated carbon fiber for direct removal of iodine from acetic acid solution, Ind. Eng. Chem. Res., 32 (2015) 1692–1697.

[21] M.S. Shafeeyan, A. Houshmand, A. Arami-Niya, H. Razaghizadeh, W.M.A.W. Daud, Modification of activated carbon using nitration followed by reduction for carbon dioxide capture, Bull. Korean Chem. Soc., 36 (2015) 533–538.

[22] A. Houshmand, D.W.M.A. Wan, S.M. Saleh, Tailoring the surface chemistry of activated carbon by nitric acid: study

using response surface method, Bull. Chem. Soc. Jpn., 84 (2011) 1251–1260.
[23] T. Yoda, K. Shibuya, K. Miura, H. Myoubudani, Characterization of the adsorption ability of silk-derived activated carbon fibers using X-ray analysis and camera imaging methods, Measurement, 101 (2017) 103–110.
[24] W. Zheng, J. Hu, S. Rappeport, Z. Zheng, Z. Wang, Z. Han, J. Langer, J. Economy, Activated carbon fiber composites for gas phase ammonia adsorption, Microporous Mesoporous Mater., 234 (2016) 146–154.
[25] R. R, J. T, R.K. G, S. Jacob, R. R, B.K. George, Adsorption performance of packed bed column for the removal of perchlorate using modified activated carbon, Process Saf. Environ., 117 (2018) 350–362.
[26] K.K. Beltrame, A.L. Cazetta, P.S. De, L. Spessato, T.L. Silva, V.C. Almeida, Adsorption of caffeine on mesoporous activated carbon fibers prepared from pineapple plant leaves, Ecotoxicol. Environ. Saf., 147 (2017) 64–71.
[27] G.B. Baur, I. Yuranov, L. Kiwi-Minsker, Activated carbon fibers modified by metal oxide as effective structured adsorbents for acetaldehyde, Catal. Today, 249 (2015) 252–258.
[28] P. He, L. Jia, G. Ma, R. Wang, J. Yuan, X. Duan, Z. Yang, D. Jia, Effects of fiber contents on the mechanical and microwave absorbent properties of carbon fiber felt reinforced geopolymer composites, Ceram. Int., 44 (2018) 10726–10734.
[29] J.M. Yuan, Z.F. Fan, Q.C. Yang, W. Li, Z.J. Wu, Surface modification of carbon fibers by microwave etching for epoxy resin composite, Compos. Sci. Technol., 164 (2018) 222–228.
[30] X. Wang, Y. Sheng, Influence of Activated Carbon Fiber Modification on Cu~(2+) Adsorption, Environ. Sci. Manage., 37 (2012) 94–96.
[31] M.E. Parolo, M.C. Savini, J.M. Vallés, M.T. Baschini, M.J. Avena, Tetracycline adsorption on montmorillonite: pH and ionic strength effects, Appl. Clay Sci., 40 (2008) 179–186.
[32] A.Y. Abdolmaleki, H. Zilouei, S.N. Khorasani, K. Zargoosh, Adsorption of tetracycline from water using glutaraldehyde-crosslinked electrospun nanofibers of chitosan/poly(vinyl alcohol), Water Sci. Technol., 77 (2018) 1324–1335.
[33] R.L. Tseng, F.C. Wu, R.S. Juang, Characteristics and applications of the Lagergren's first-order equation for adsorption kinetics, J. Taiwan Inst. Chem. Eng., 41 (2010) 661–669.
[34] M.I. El-Khaiary, G.F. Malash, Y.S. Ho, On the use of linearized pseudo-second-order kinetic equations for modeling adsorption systems, Desalination, 257 (2010) 93–101.
[35] N. Ghasemi, P. Tamri, A. Khademi, N.S. Nezhad, S.R.W. Alwi, Linearized equations of pseudo second-order kinetic for the adsorption of Pb(II) on Pistacia Atlantica shells, Ieri. Procedia., 5 (2013) 232–237.
[36] F.C. Wu, T. Ruling, J. Rueyshin, Characteristics of Elovich equation used for the analysis of adsorption kinetics in dye-chitosan systems, Chem. Eng. J., 150 (2009) 366–373.
[37] M. Rasouli, N. Yaghobi, M. Hafezi, M. Rasouli, Adsorption of divalent lead ions from aqueous solution using low silica nano-zeolite X, J. Ind. Eng. Chem., 18 (2012) 1970–1976.
[38] R.M. Ali, H.A. Hamad, M.M. Hussein, G.F. Malash, Potential of using green adsorbent of heavy metal removal from aqueous solutions: Adsorption kinetics, isotherm, thermodynamic, mechanism and economic analysis, Ecol. Eng., 91 (2016) 317–332.
[39] S. Brunauer, P.H. Emmett, Chemisorptions of gases on iron synthetic ammonia catalysts, J. Am. Chem. Soc., 62 (1940) 1732–1746.
[40] A. Li, S. Pi, W. Wei, T. Chen, J. Yang, F. Ma, Adsorption behavior of tetracycline by extracellular polymeric substrates extracted from Klebsiella sp., Environ. Sci. Pollut. Res. Int., 23 (2016) 25084–25092.
[41] N. Rattanachueskul, A. Saning, S. Kaowphong, N. Chumha, L. Chuenchom, Magnetic carbon composites with a hierarchical structure for adsorption of tetracycline, prepared from sugarcane bagasse via hydrothermal carbonization coupled with simple heat treatment process, Bioresour. Technol., 226 (2017) 164–172.
[42] S. Vilvanathan, S. Shanthakumar, Removal of Ni(II) and Co(II) ions from aqueous solution using teak (Tectona grandis) leaves powder: adsorption kinetics, equilibrium and thermodynamics study, Desal. Wat. Treat., 57 (2016) 3995–4007.
[43] A. Chatterjee, S. Schiewer, Multi-resistance kinetic models for biosorption of Cd by raw and immobilized citrus peels in batch and packed-bed columns, Chem. Eng. J., 244 (2014) 105–116.
[44] W.F. Liu, Z. Jian, C.L. Zhang, Y. Wang, L. Ye, Adsorptive removal of Cr (VI) by Fe-modified activated carbon prepared from Trapa natans husk, Chem. Eng. J., 162 (2010) 677–684.
[45] A.K. Alegakis, M.N. Tzatzarakis, A.M. Tsatsakis, I.G. Vlachonikolis, V. Liakou, In vitro study of oxytetracycline adsorption on activated charcoal, J. Environ. Sci. Health., Part B, 35 (2000) 559–569.
[46] M. Harja, G. Ciobanu, Studies on adsorption of oxytetracycline from aqueous solutions onto hydroxyapatite, Sci. Total Environ., 628–629 (2018) 36–43.
[47] G. Feng, Yang, Adsorption and desorption of oxytetracycline in four constructed wetland substrates, Chinese. J. Environ. Eng., 7 (2013) 1683–1688.
[48] X. Song, D. Liu, G. Zhang, M. Frigon, X. Meng, K. Li, Adsorption mechanisms and the effect of oxytetracycline on activated sludge, Bioresour. Technol., 151 (2014) 428–431.